

Cover Page



Universiteit Leiden



The handle <http://hdl.handle.net/1887/25579> holds various files of this Leiden University dissertation

Author: Driessen, R. P. C.

Title: The architects of crenarchaeal chromatin : a biophysical characterization of chromatin proteins from *Sulfolobus solfataricus*

Issue Date: 2014-05-06

CHAPTER 3

Tethered Particle Motion reveals how temperature affects DNA flexibility and protein-DNA interactions

This chapter has been submitted for publication

Rosalie P.C. Driessen, Gerrit Sitters, Niels Laurens, Geri F. Moolenaar, Gijs J.
L. Wuite, Nora Goosen, Remus Th. Dame

ABSTRACT

The helical structure of double stranded DNA is destabilized by increasing temperature. Above a critical temperature (the melting temperature) the two strands in duplex DNA become fully separated. Below this temperature the structural effects are localized. Using Tethered Particle Motion in a temperature-controlled sample chamber, we systematically investigate the effect of increasing temperature on DNA structure and the interplay between this effect and protein binding. Our measurements reveal 1) that increasing temperature enhances DNA flexibility, effectively leading to more compact folding of the double stranded DNA chain and 2) that this effect on DNA structure differentially affects different types of DNA-bending chromatin proteins from mesophilic and thermophilic unicellular organisms. Thus, our findings are key to understanding genome organization in organisms thriving at moderate as well as extreme temperatures. Moreover, our results underscore the importance of carefully controlling and measuring temperature in single-molecule DNA (micromanipulation) experiments.

INTRODUCTION

Double stranded DNA (dsDNA) is a semi-flexible polymer (226). On short length scales (in the order of its persistence length: ~ 150 basepairs or ~ 50 nm) stiffness dominates its conformation and bending is energetically unfavourable. However, on the larger scale dsDNA acts as a flexible polymer and forms a random coil. Although the exact cause of DNA rigidity remains unclear, it has been proposed that both basepair stacking and the electrostatic repulsions of the negatively charged phosphate backbone contribute to the local stiffness of the DNA (226,227). In order to facilitate genome-based processes such as transcription, DNA repair and replication, the relatively stiff DNA is sharply bent on local scales (228). Despite its global flexibility genomic DNA also needs to be bent substantially to fit into the volume of a cell or cell nucleus.

Across all domains of life, cells employ small architectural proteins that bend the DNA in order to compact the genome (14). Eukaryotes and many archaeal species express histone proteins that sharply bend and wrap DNA into compacted nucleosomes (34,45,52). Other nucleoid-associated proteins have been shown to induce compaction by local DNA bending. Examples include the eukaryotic high mobility group (HMG) proteins (194), the bacterial DNA bending proteins HU, IHF and Fis (36,37), and the crenarchaeal proteins Sul7 and Cren7 (229). Besides the role of DNA-bending proteins in genome compaction and organization, the bending induced by these proteins is also crucial in regulatory processes (230). Regulatory complexes *in vivo* often involve the formation of small DNA loops (231) which require sharp bending of DNA. A mechanism to enhance the formation and stability of these loops is the binding of a DNA bending protein within the loop. For example, HU was shown to stabilize various kinds of repression loops (among which loops mediated by the bacterial Lac and Gal repressor) by enhancing DNA flexibility (170,171). In the Gal repressosome two GalR dimers form a small loop facilitated by the binding of an HU dimer at the apex of the loop (172). Other studies have shown that

sharp bending of DNA can occur spontaneously, yielding a higher intrinsic bendability of DNA on short length scales compared to long length scales (232,233). Such strong bending of short dsDNA is caused either by the formation of small melting bubbles or transient kinks (234-238). Based on the observation that sharp bending of DNA occurs spontaneously it was suggested that DNA flexibility itself acts as a factor affecting the conformation and stability of looped regulatory complexes *in vivo* (239).

It is likely that the flexibility and bendability of DNA affect spatial genome folding and functioning. Indeed it has been shown in biochemical ensemble measurements that temperature directly affects DNA structure by changing its persistence length (240). Besides such a direct effect on DNA structure, temperature might also influence the interactions between DNA and architectural proteins, and hence chromatin structure. Growth temperature and fluctuations in this temperature are thus expected to have a strong impact on *in vivo* DNA organization and gene regulation. Indeed, the transcription of many genes changes following moderate temperature shifts in both mesophilic *E. coli* (241) as well as thermophilic *S. solfataricus* (242). In addition to being associated with a general stress response (243), such effects on transcription could in part be mediated by global changes in chromatin structure due to the change in temperature. Single-molecule experiments concerning DNA flexibility and protein-DNA interactions are generally conducted at room temperature. However, the large majority of organisms lives at temperatures different from room temperature: psychrophiles thrive at temperatures around 0 °C, mesophiles at 20 – 45 °C, while thermophilic organisms live at temperatures up to ~ 100 °C. In this study, we investigate the effect of temperature on DNA structure and flexibility at temperatures ranging from 23 – 52 °C using a temperature controlled tethered particle motion (TPM) set-up. Moreover, we investigate the effect of temperature on the binding and bending behaviour of the architectural proteins Cren7 and Sul7 from the thermophilic organism *S. solfataricus* (living at temperatures between 40 and 90 °C) and HU from mesophilic *E. coli* (living at temperatures between 10 and 40 °C).

RESULTS

Increasing temperature enhances DNA flexibility

The motivation of our studies is to study protein-DNA interactions at temperatures relevant for the organisms encoding these proteins. Such interactions might be affected by changes in structure and DNA flexibility occurring by changing temperature. To investigate the direct effect of temperature on DNA structure and flexibility we performed Tethered Particle Motion (TPM) experiments over a range of temperatures. Since the physical properties of dsDNA are dependent on the basepair composition (244), we measured three different DNA constructs of identical length (685 bps) but different average GC content (32%, 53% and 70%). Using bulk DNA melting measurements we first determined the melting temperatures (T_m) to be $T_{m,32\%} = 76.8 \pm 0.5$ °C, $T_{m,53\%} = 84.9 \pm 0.5$ °C and $T_{m,70\%} = 91.2 \pm 0.5$ °C for the substrate with 32%, 53% and 70% GC basepairs respectively (see Figure S3.1).

In our TPM experiments we focus on the local effects of temperature on global DNA conformation by measuring at temperatures below the melting temperature of all three DNA substrates ($T = 23 - 52$ °C). We probed the conformational state of many individual DNA molecules in this range of temperatures by tracking the excursion of the attached bead (quantified by the root mean square (RMS) value of its excursion). If the length of a tether is not changed, the RMS of the attached bead is a measure of its apparent persistence length; a tether attains a more compact formation if it becomes more flexible or if it is locally bent by a ligand (see Figure 3.1 A). At 23 °C, the measured RMS values ranged from $RMS = 157.2 \pm 0.5$ nm (error represents standard error of the mean (SE)) for the 32% GC substrate to $RMS = 161.4 \pm 0.7$ nm for the 70% GC substrate. DNA with a higher GC content yielded a slightly higher RMS value, due to an on average somewhat less flexible DNA substrate. Increasing the temperature caused the RMS values of all DNA tethers to decrease (see Figure 3.2 A), pointing to an increase in flexibility.

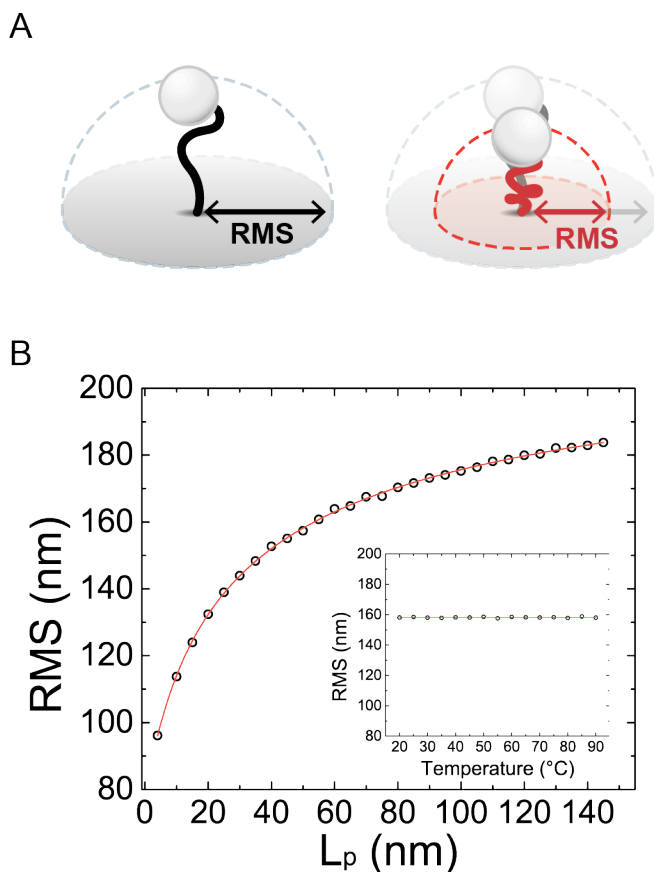


Figure 3.1 RMS is a measure for DNA persistence length. **A.** Schematic representation of a TPM experiment. *Left:* The RMS value quantifies the excursion of a bead attached to a single DNA molecule, tethered to the surface of the flow cell. *Right:* As the persistence length decreases, the DNA molecule will be in a more compact configuration (*red DNA molecule*), which leads to a smaller RMS value. **B.** RMS dependence on persistence length L_p obtained from bead movement simulations ($L_0 = 233$ nm and $d_{\text{bead}} = 460$ nm) fitted with Equation (3.1). Inset shows that the bead movement (RMS) itself is not affected by temperature when DNA parameters are kept constant ($L_0 = 233$ nm, $L_p = 50$ nm and $d_{\text{bead}} = 460$ nm).

To quantitatively relate the measured RMS values to the physical properties of the DNA, we performed numerical simulations describing the movement of the bead as a function of DNA persistence length L_p . The RMS of the simulated tethered beads was calculated from the x and y positions obtained from the simulations (see Materials and Methods). Figure 3.1 B shows the relation between the persistence length and the measured RMS value for a tether with contour length $L_0 = 233$ nm (685 bps) and bead diameter $d_{\text{bead}} = 460$ nm. By fitting the results with a hyperbola function, we obtained the following empirical relation between L_p and RMS:

$$\text{RMS} = 233 - \frac{156}{(1 + 0.08 \cdot L_p)^{0.45}} \quad (3.1)$$

To validate our approach and to ensure that the measured change in RMS is exclusively due to changes in flexibility of the DNA, we tested if the temperature has an effect on the bead motion itself. In our simulations a change in temperature may affect the movement of the bead by influencing the viscosity of the solution and the thermal fluctuations on the bead and the DNA. Despite these temperature effects, the bead movement ($L_0 = 233$ nm, $L_p = 50$ nm and $d_{\text{bead}} = 460$ nm) yielded a constant RMS value at different temperatures (see inset Figure 3.1 B), which indicates that the RMS itself is not influenced by temperature within a range of 20 – 90 °C. This confirms that the measured RMS is dependent only on the physical properties of the DNA, which we can describe as a function of apparent persistence length according to Equation (3.1). The apparent persistence length of the DNA molecule is a measure for the average flexibility of a heterogeneous chain (192,196).

Using Equation (3.1) we calculated the apparent persistence length of the DNA substrates within the measured temperature range. Figure 3.2 B shows that the apparent persistence length scales linearly with temperature within this temperature range. Linear fitting of the data ($L_p = L_p^0 - C \cdot T$) yielded a temperature dependence of the persistence length (C), which is

slightly dependent on the GC percentage of the DNA substrate (see Table 3.1). L_p^0 denotes the apparent persistence length at $T = 0$ °C, but as water will freeze around this temperature, this linear dependence is not valid at temperatures close to $T = 0$ °C. The generic effect of temperature on DNA flexibility is in agreement with recent magnetic tweezer studies (245,246). The observed linear dependence of apparent persistence length on temperature is in good qualitative agreement with the work of Geggier *et al.* (240), in which cyclization of short DNA fragments was investigated in the range of 5 – 42 °C in ensemble measurements.

Table 3.1 Temperature dependent DNA properties of DNA substrates (685 bp) with different GC content.

GC content	C (nm/ °C)	L_p^0 (nm)	T_m (°C)
32%	0.66 ± 0.05	62.7 ± 1.9	76.8 ± 0.5
53%	0.79 ± 0.05	71.2 ± 2.3	84.9 ± 0.5
70%	0.82 ± 0.03	74.9 ± 1.2	91.2 ± 0.5

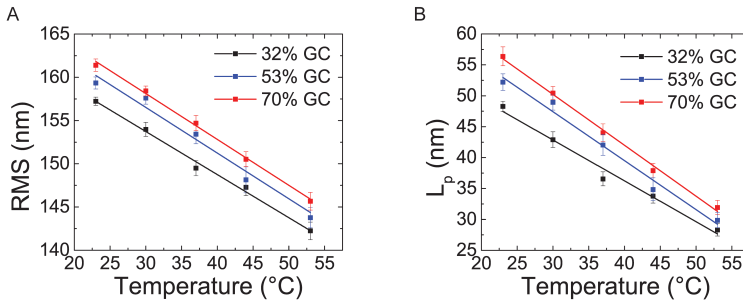


Figure 3.2 Temperature dependent DNA flexibility **A.** RMS distances of dsDNA molecules (685 bp) with a GC percentage of 32%, 53% and 70% as a function of temperature. Error bars represent the standard error of the mean ($N = 58 - 352$) **B.** Apparent persistence length of all three substrates as a function of temperature. L_p is calculated from data showed in A. according to Equation (3.1). Lines show a linear fit (see Table 3.1 for fitting parameters).

Influence of temperature on the binding and bending of DNA bending proteins

A higher flexibility of DNA at higher temperatures could be an important element contributing to DNA organization and dynamics in organisms with high growth temperatures. As the apparent persistence length of DNA is reduced by increasing temperature, the conformation of the molecule becomes more compact independent of architectural protein binding. In addition to such a direct effect of temperature on the intrinsic properties of DNA, the interaction between architectural proteins and DNA might also be affected by temperature. However, single-molecule experiments concerning protein-DNA interactions of architectural proteins have been traditionally conducted at room temperature.

To determine the architectural properties of such proteins under conditions more relevant for the *in vivo* situation, we investigated the effects of the DNA bending proteins Cren7 and Sul7 from thermophilic *S. solfataricus* and HU from mesophilic *E. coli* on DNA structure at physiological temperatures. *Sulfolobus* species (40,229) live at temperatures in the range of 40 – 90 °C (17). The Cren7 and Sul7 proteins encoded by these organisms are structural homologues, both inducing rigid bends upon binding to DNA (90) by intercalating into the minor groove (97,101). Our earlier single-molecule micromanipulation experiments performed at room temperature (~ 23 °C) revealed that this bending results in a decrease of apparent persistence length and thus compaction of DNA molecules (90). DNA melting experiments revealed that both Cren7 and Sul7 increase the melting temperature (63,70), which might imply an important role for these proteins in maintaining DNA integrity at high temperatures. To determine how the interaction of Cren7 and Sul7 with DNA is affected by temperature in the sub-melting regime in which DNA becomes more flexible, we performed TPM experiments at both 23 °C and 52 °C. For these studies we used the 32% GC substrate, which is representative for the average GC content of the *S. solfataricus* genome (22). The persistence length L_p for

protein concentrations of 0 – 1600 nM for both Cren7 and Sul7 at 23 °C and 52 °C, calculated from the measured RMS values using Equation (3.1) is shown in Figure 3.3 A and B. At 23 °C both proteins reach a minimum persistence length of ~ 10 nm, which is consistent with our earlier measurements using magnetic tweezers conducted at this temperature (90). This agreement further validates our approach of converting RMS values into values for persistence length L_p . At 52 °C (*red data points*) compaction sets in at lower protein concentrations than at 23 °C (*black data points*), but the maximum level of compaction achieved at both temperatures is comparable. At high protein concentrations, when the DNA is saturated with protein the change in temperature does not measurably influence the conformation of the protein-DNA complexes.

To quantitatively compare the binding affinities of the proteins at the different temperatures, we calculated the fractional coverage (ν) of the DNA as follows (178):

$$\nu = \frac{\sqrt{\frac{1}{L_p}} - \sqrt{\frac{1}{L_{p,\text{bare}}}}}{\sqrt{\frac{1}{L_{p,\text{saturated}}}} - \sqrt{\frac{1}{L_{p,\text{bare}}}}} \quad (3.2)$$

where L_p represents the measured persistence length, $L_{p,\text{saturated}}$ the minimum persistence length at saturation and $L_{p,\text{bare}}$ the persistence length of bare DNA. In this approach it is assumed that each bound protein has an equal contribution to the decrease in DNA stiffness. Figure 3.3 C and D show the fractional coverage as a function of protein concentration.

To calculate binding affinities under the different conditions, the fractional coverage was fitted to the McGhee and von Hippel theory (247). This model describes protein binding to DNA in terms of the association constant (K), a cooperativity parameter (ω) and the protein binding site (n). Using a footprint of $n = 8$ bp for both proteins (95,101), we obtained fitting

parameters for K and ω . Both Cren7 and Sul7 show an increase in binding affinity at 52 °C compared to 23 °C. The association constant found for Cren7 was $K_{\text{Cren},23} = (2.5 \pm 0.2) \cdot 10^5 \text{ nM}^{-1}$ at room temperature (23 °C) and increased to $K_{\text{Cren},52} = (7.4 \pm 1.4) \cdot 10^5 \text{ nM}^{-1}$ at 52 °C. The cooperativity factor of $\omega_{\text{Cren},23} = 18.8 \pm 3.2$, indicates low cooperativity in binding, which is somewhat affected by the increase of temperature as $\omega_{\text{Cren},52} = 10.4 \pm 3.6$. Sul7 exhibits a lower DNA binding affinity compared to Cren7 as $K_{\text{Sul},23} = (1.3 \pm 0.3) \cdot 10^5 \text{ nM}^{-1}$ at 23 °C and $K_{\text{Sul},52} = (1.8 \pm 0.2) \cdot 10^5 \text{ nM}^{-1}$ at 52 °C, yielding a slightly higher binding affinity at 52 °C. Similar to Cren7 the cooperativity in binding of Sul7 to DNA is essential independent of temperature: $\omega_{\text{Sul},23} = 8.4 \pm 2.4$ and $\omega_{\text{Sul},52} = 8.1 \pm 2.0$.

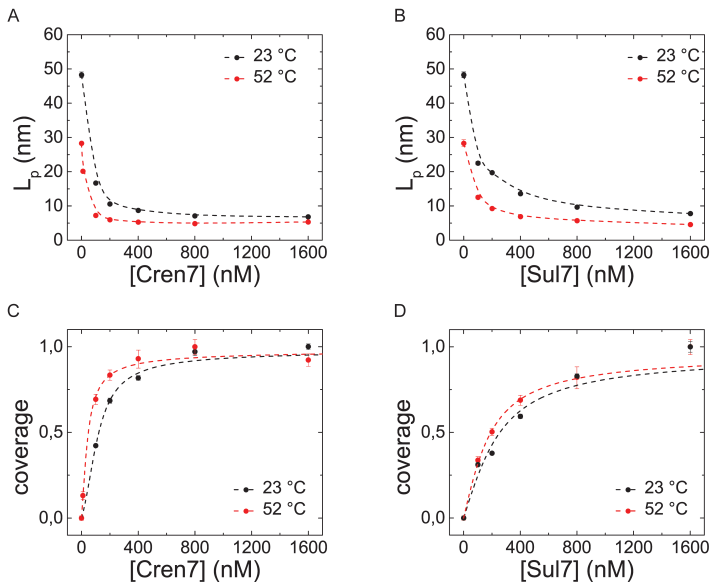


Figure 3.3 Apparent persistence length as a function of protein concentration of **A.** Cren7 and **B.** Sul7 at 23 °C and 52 °C. **C and D.** Fractional coverage as a function of protein concentration, calculated according to Equation (3.2) from data showed in A and B. Fitting the coverage to the McGhee- von Hippel theory showed that binding affinity is increased at 52 °C: $K_{\text{Cren},23} = (2.5 \pm 0.2) \cdot 10^5 \text{ nM}^{-1}$ and $K_{\text{Cren},52} = (7.4 \pm 1.4) \cdot 10^5 \text{ nM}^{-1}$ and $K_{\text{Sul},23} = (1.3 \pm 0.3) \cdot 10^5 \text{ nM}^{-1}$ and $K_{\text{Sul},52} = (1.8 \pm 0.2) \cdot 10^5 \text{ nM}^{-1}$ for Sul7. Error bars represent the standard error of the mean ($N = 69 - 352$).

To investigate whether the effect of temperature on DNA binding shown for Cren7 and Sul7 is generic for DNA bending proteins, we performed similar experiments with the bacterial chromatin protein HU, the most abundant DNA bending protein in *E. coli*. It exhibits two different DNA binding modes depending on the stoichiometry: DNA bending and compaction at low protein concentrations and DNA stiffening at high protein concentrations (195,196,248). TPM measurements performed at 23 °C show that HU induces compaction by reducing the apparent persistence length to a minimum of $L_p = 12.9 \pm 0.2$ nm at a protein concentration of 400 nM (see Figure 3.4). At HU concentrations > 400 nM the persistence length increases up to $L_p = 20.1 \pm 0.4$ nm at a protein concentration of 1600 nM reflecting the transition into the stiffening mode. In this concentration regime, HU proteins bind side-by-side forming filaments, which stabilizes the DNA helix (249). We did not observe an increase of the persistence length above that of bare DNA as observed in previous micromanipulation experiments of single HU-DNA complexes (195,196). However, previously reported TPM experiments exhibited a similar trend: the persistence length increases at high HU concentrations, but does not exceed the persistence length of bare DNA molecules (248). Possibly, the force applied in the previous DNA micromanipulation experiments facilitates the transition into the stiffening mode of HU, giving rise to the apparent discrepancy in observed persistence lengths.

Next, we carried out TPM measurements for the same protein concentration range at 37 °C, the optimum growth temperature of *E. coli*. Surprisingly, a temperature increase of only 14 °C had a large effect on the measured apparent persistence length. Although the maximum level of compaction was achieved at a similar protein concentration (400 nM), the persistence length at this concentration was reduced significantly to $L_p = 6.1 \pm 0.2$ nm at 37 °C. In the stiffening regime (> 400 nM) the persistence length increased slightly to $L_p = 10.7 \pm 0.3$ nm at 1600 nM, indicating that the DNA stiffening still occurs in this regime at 37 °C. As the maximum level of compaction is achieved at the same protein concentration, the

affinity of HU for DNA is not affected by the change in temperature from 23 to 37 °C. The change in temperature did however significantly enhance the degree of compaction induced by HU, suggesting that the degree of bending induced by HU is increased at 37 °C.

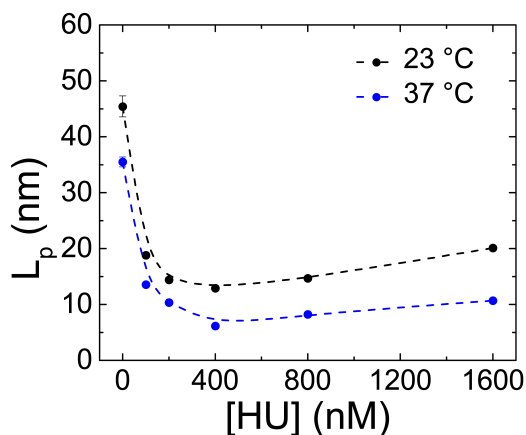


Figure 3.4 Apparent persistence length as a function of HU concentration at 23 °C (black) and 37 °C (blue). Compaction is increased at 37 °C. Error bars represent the standard error of the mean (N = 52 – 236).

DISCUSSION

Our single-molecule TPM experiments reveal that the flexibility of DNA strongly depends on temperature in the range of 23 – 52 °C. The temperature coefficient of the persistence length (C) is slightly dependent on GC content of the DNA substrate and ranges from $C = 0.66 \pm 0.05$ nm/°C for the DNA substrate with an average GC content of 32% to $C = 0.82 \pm 0.03$ nm/°C for the substrate with 70% GC content. Although the temperature effect on the apparent persistence length observed in our study is much more pronounced than in previous work by Geggier *et al.* (240), the observed trend is similar: increased temperature lowers the resistance to bending of the DNA. What causes such a strong temperature dependence

on the L_p remains unclear. Thermal stability of the dsDNA helix involves base pair interactions between bases of complementary strands and base-stacking interactions between adjacent bases. Although Yakovchuk *et al.* (250) found that the base-stacking interactions are the dominant factor in stabilizing the double-stranded helix, they did not show how this relates to the bending rigidity of the DNA. A recent study addressed this question by measuring mechanical properties of chemically modified DNA molecules, with altered charge or base stacking interactions (251). This revealed that stacking interactions do not straightforwardly correlate with the mechanical properties of DNA, such as the persistence length. It is thus unlikely that stacking interactions alone cause such a pronounced temperature dependent persistence length. Spontaneous sharp bending of dsDNA has been explained in different models involving kinks (caused by unstacking of adjacent basepairs) or small melting bubbles (disrupted base pairing and/or base stacking). Probably increasing temperature enhances both of these processes, strongly influencing the apparent persistence length (as observed in our experiments). A recent theoretical study indeed suggests a model that describes the experimentally observed temperature dependent DNA persistence length as a function of both an isotropic temperature dependent bending stiffness of the dsDNA helix and small local melting bubbles (252).

The fact that the flexibility of dsDNA strongly depends on temperature has important implications for genome conformation *in vivo*. Organisms will experience different mechanical properties of DNA depending on the temperature of their natural habitat. As temperature increases the bendability of dsDNA, organisms living at elevated temperatures could benefit from this increased bendability in the light of genome compaction. The persistence length directly relates to the size of an unconstrained dsDNA molecule in solution, typically quantified by the so-called radius of gyration (R_g). For instance, the genome of an archaeal or bacterial cell is in the order of millimeters in length which corresponds to $R_g \approx 4 \mu\text{m}$ at $T = 25 \text{ }^\circ\text{C}$ ($L_p = 50 \text{ nm}$). A change in temperature to $52 \text{ }^\circ\text{C}$ would reduce the radius of gyration of a genome of that length to $R_g \approx 3.2 \mu\text{m}$ (a reduction in

effective volume by about 25%). Temperature itself could thus serve as a mechanism to modulate the compaction levels of genomic DNA. It is therefore an important aspect to consider when studying *in vivo* chromatin organization and compaction of thermophilic organisms and psychrophilic organisms living at temperatures that differ from room temperature.

Our results show that temperature not only affects the intrinsic properties of DNA, but also influences protein-DNA interactions of DNA-bending proteins. Interestingly, this temperature dependence is not shared among the different DNA-bending proteins investigated; it seems to depend on the nature of the protein-DNA interactions. Both Cren7 and Sul7 from thermophilic *S. solfataricus* exhibit an increased binding affinity at an elevated temperature of 52 °C. Increased binding affinity at higher temperatures was shown before for Sul7 by isothermal titration calorimetry (ITC) (253). In these ITC studies the binding affinity for poly(dGdC) increased about 5 fold when increasing the temperature from 25 °C to 80 °C. Molecular dynamics simulations of Cren7 also showed an increased affinity at elevated temperatures (104). The increase in binding affinity could be attributed to the increased flexibility of DNA at higher temperatures, which lowers the energy barrier to induce DNA bending. Another mechanism, that could contribute to an increased affinity, is that transient melting bubbles make the DNA more accessible for binding of Cren7 and Sul7, as these proteins intercalate into the minor groove of DNA.

In contrast with Cren7 and Sul7, the DNA-bending protein HU from mesophilic *E.coli* did not show an increased binding affinity upon a temperature increase of $\Delta T = 14$ °C. Instead, HU binding at 37 °C resulted in significantly enhanced compaction. Previous studies, performed at room temperature, have shown that HU induces flexible bends, which can range from 0 – 180° with equal probability (196,209). An increase in temperature could bias the bending angle distribution towards higher bending angles as the energy barrier required to bend the DNA is decreased. The observed increase in compaction could thus be a result of enhanced bending at

higher temperature. At 37 °C the bimodal behavior of HU still persisted: the observed compaction reached a maximum at 400 nM and at concentrations > 400 nM the apparent persistence length increased. The stiffening regime is however less pronounced compared to 23 °C as the apparent persistence length reached a maximum of $L_p = 10.7 \pm 0.3$ nm at 1600 nM (compared to $L_p = 20.1 \pm 0.4$ nm at 23 °C). As the molecular mechanism underlying the stiffening mode is not understood, it is difficult to explain what causes the difference in stiffening at different temperatures. Possibly, the increased flexibility of the DNA at 37 °C effectively counteracts the stiffening effect of the HU filaments. Also, protein-protein interactions could be affected by temperature, influencing the side-by-side binding of HU proteins, which causes the observed stiffening. A smaller distribution of bending angles could also cause a less tight packing of the proteins on the DNA within the stiffening regime, causing a less pronounced stiffening effect, as observed. Indeed it has been suggested that a flexible bending angle is needed for tight packing of proteins along the DNA (90).

The increase in flexibility of DNA at increased physiologically relevant temperatures is important when aiming to understand chromatin organization *in vivo*. It does not only lead to a more compact configuration of the genomic DNA, but can also have an important effect on cellular processes such as gene regulation. As DNA structure and topology are temperature dependent this may affect gene expression on a global level (254). DNA supercoiling is proposed to act as a global regulator as it changes in response to environmental conditions and affects the expression of many genes (162). Analogous to supercoiling, temperature dependent DNA flexibility (and associated local changes in twist) and global compaction could provide a mechanism for temperature sensitive gene regulation.

MATERIALS AND METHODS

Protein purification

Cren7 was purified as described before (90). Sul7 was purified from *E. coli* strain BL21-CodonPlus(DE3) containing plasmid pRD26 (a pET11A derivative containing the gene encoding Sul7 (gene SSO10610) from *S. solfataricus*). Cells were grown in LB medium up to $OD_{600} \approx 0.4$, and expression was induced using 0.5 mM IPTG at 37 °C. Two hours after induction, cells were harvested by centrifugation and resuspended in 20 ml buffer A [50 mM Tris-HCl (pH 8.0), 2 mM $MgCl_2$, 0.1% Triton X100, 386 $\mu\text{g/ml}$ benzamidine hydrochloride, 10 mM β -mercaptoethanol]. Cells were lysed by sonication, 1000 units OmniCleave Endonuclease (Westburg) per gram cells was added and the cell lysate was incubated for 30 min at room temperature. After heating the cell lysate for 40 min at 70 °C, 1 ml of 0.5 M EDTA was added. The cell lysate was centrifuged for 30 min at 37,000 r.p.m. and filtered through a 0.45 μm membrane filter (MiliPore). The supernatant was applied to a HiTrap-S column (GE Healthcare), equilibrated in buffer B [10 mM KPO_4 (pH 7.0), 10% glycerol]. Protein was eluted with a linear gradient of 0 – 1 M NaCl in buffer B. Cren7 and Sul7 proteins were dialyzed at 4 °C against a storage buffer [20 mM HEPES (pH 7.5), 100 mM NaCl, 10% Glycerol, 10 mM β -mercaptoethanol], and stored at -80 °C until required. Protein concentrations were determined using a Bicinchoninic Acid (BCA) protein Assay (Thermo Scientific). HU protein was purified as described before (255).

DNA constructs

End-labeled DNA constructs of 685 bp with different GC content (32%, 53% and 70% GC) were generated by PCR using plasmids pRD118, pNP83 (256) and pBTH154 as templates and biotin- and digoxigenin-labeled primers (designed to specifically yield a product of the desired length based on the sequences cloned into these plasmids). pRD118 was constructed by inserting a 685 bp long fragment from the *S. solfataricus* P2 genome (22)

into the NdeI and BamHI site of pET3-his (257). pBTH154 was constructed by inserting the dasR gene (SCO5231) of the *Streptomyces coelicolor* A3 (2) (258) into the XbaI and XmaI site of pUT18C (Euromedex). All PCR products were purified using a GenElute PCR Clean-up kit (Sigma-Aldrich). DNA substrates were checked for local GC percentage and predicted curvature (see Figure S3.2) to ensure the variation is small and to prevent local curvature dominating the global flexibility of the substrates. DNA substrates used for the bulk melting experiments were obtained following the same approach with unlabeled primers.

Bulk melting curves

Melting curves of the three DNA substrates with different GC-content (see above) were measured using a Varian Cary300Bio UV-Vis spectrophotometer, measuring ultraviolet absorbance at $\lambda = 260$ nm. DNA was diluted to a final concentration of 4 $\mu\text{g/ml}$ in a buffer containing 10 mM HEPES (pH 7.5) and 100 mM NaCl. Temperature was increased with a rate of 1 $^{\circ}\text{C}/\text{min}$ within a range of 25 – 95 $^{\circ}\text{C}$. The melting temperature T_m is defined as the temperature at which half of the dsDNA is dissociated into ssDNA, which equals the temperature at which the slope of the melting curve is at its maximum. To determine the T_m the first derivative was calculated and the peak position (corresponding to the T_m) was determined by fitting a Gaussian distribution.

Tethered particle motion experiments

Flow cells (volume ~ 30 μl) were incubated with 20 $\mu\text{g/ml}$ anti-DIG antibodies (Roche) and for 5 min. Passivation of the surface was achieved by flushing the flow cell with 0.4% (w/v) Blotting Grade Blocker (BGB) (Bio-Rad) in buffer I [10 mM Tris (pH 7.5), 150 mM NaCl, 1 mM EDTA, 1 mM DTT, 3% glycerol, 100 $\mu\text{g/ml}$ acetylated BSA (Ambion)] and incubating for 15 min at the desired temperature (23 – 52 $^{\circ}\text{C}$). The flow cell was flushed with buffer I, filled with 200 pM DNA solution (functionalized with biotin and DIG) and incubated for 10 min. and flushed again with buffer I.

Streptavidin coated polystyrene beads with a diameter of 0.46 μm (1% w/v; G Kisker) were diluted 300 times in buffer I, flushed into the flow cell and incubated for 10 min to allow binding to the biotin-ends of the DNA. The flow cell was washed with protein diluted in buffer II (10 mM HEPES (pH 7.5), 100 mM NaCl, 0.2% (w/v) BGB) for Cren7 and Sul7 or buffer III (20 mM HEPES (pH 7.9), 60 mM KCl, 0.2% (w/v) BGB) for HU. After flowing in the final incubation solution with or without protein the flow cell was closed and incubated at the desired temperature (23 – 52 $^{\circ}\text{C}$) for 10 min before starting measurements. Experiments without protein were all done in buffer II.

Tethered particle motion experiments were performed on an inverted Nikon microscope (Diaphot 300), using a 100x oil-immersion objective (NA = 1.25). To control the temperature of the flow cell, a custom-built temperature control system was implemented by placing heating elements around the objective and inside the flow cell holder. Using a calibrated temperature probe the accuracy of the temperature set on the controller was verified in the area directly above the objective. Next, a feedback system was used to secure constant temperature within ± 1 $^{\circ}\text{C}$. The sample stage was isolated to avoid temperature drift within the sample. Images were acquired using a CMOS camera (Thorlabs) at 25 Hz. The x- and y- coordinates of individual beads were tracked real-time by custom-developed LabView software (National Instruments) as described previously (259).

Data Analysis

The root mean square (RMS) value of the excursion of each individual bead was calculated from x- and y-coordinates of a 40 s time trace (corrected for linear drift) by $\text{RMS} = \sqrt{\langle (x - \bar{x})^2 + (y - \bar{y})^2 \rangle}$, where \bar{x} and \bar{y} are averaged over the full time trace. Symmetry of the excursion of the tethered beads was evaluated by calculating the anisotropic ratio $a = l_{\text{major}} / l_{\text{minor}}$ from the xy-scatter plots, where l_{major} and l_{minor} represent the major and minor axis of the xy-scatter plot respectively. Fluctuations of RMS in time were quantified

by calculating the relative standard deviation of the smoothed RMS $\sigma_{rel} = \sigma_{smoothed} / \langle RMS \rangle_{smoothed}$, where $\sigma_{smoothed}$ represents the standard deviation of $RMS_{smoothed}$, which represents the RMS smoothed over a 2 s time window. Only tethers with a high symmetry $a \leq 1.14$ and small RMS fluctuations $\sigma_{rel} \leq 0.06$ were qualified as good tethers and selected for further analysis. For each measured condition RMS values were obtained by fitting a single Gaussian to the histogram of the RMS values of individual tethers ($N = 52 - 352$).

Bead movement simulations

Bead movement is simulated numerically by solving the Langevin equation for a tethered bead. This is done for both translation and rotation (260):

$$\begin{aligned} x_{n+1} &= x_n + (\gamma - 1) \cdot F_{ext} + F_{brown} \Delta t \\ \varphi_{n+1} &= \varphi_n + (\beta - 1) \cdot \Theta_{DNA} + \Theta_{brown} \Delta t \end{aligned} \quad (3-3)$$

where x_n and x_{n+1} are the bead's three dimensional position at step n and $n+1$ of the simulation respectively. The angles φ_n and φ_{n+1} denote the bead's orientation. γ and β are the effective translational and rotational drag coefficient vectors, which are calculated using Faxen's law. F_{ext} is the external force working on the bead caused by gravity, buoyancy, the surface and the DNA. Θ_{DNA} is the torque exerted on the bead caused by the DNA. The DNA is modeled by the finite WLC model assuming fully constraint boundary conditions (261). F_{brown} and Θ_{brown} are the fluctuating thermal force and torque that are described by the fluctuation-dissipation theorem and are Gaussian distributed (262). Δt is the time step of the simulation and is typically set to 1 μs . Decreasing Δt did not affect the statistical properties of the simulated traces.

SUPPLEMENTARY INFORMATION

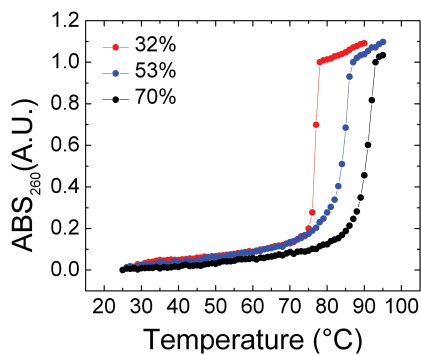


Figure S3.1 Bulk dsDNA melting curves of 685 bp fragments containing 32%, 53% and 70% GC basepairs showed melting temperatures of $T_{m,32\%} = 76.8 \pm 0.5$ °C, $T_{m,53\%} = 84.9 \pm 0.5$ °C and $T_{m,70\%} = 91.2 \pm 0.5$ °C respectively.

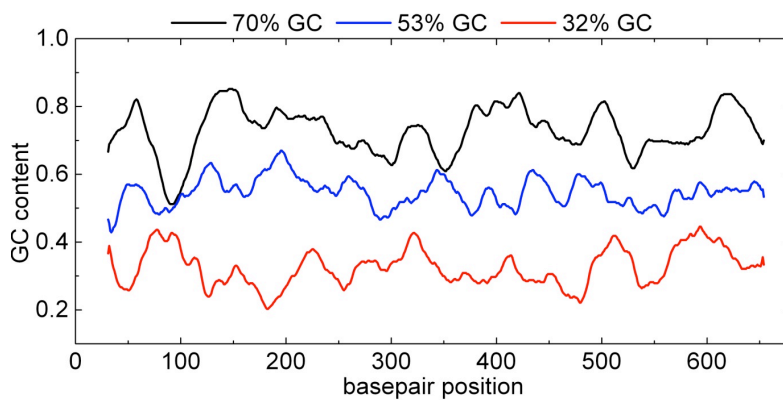


Figure S3.2 Local GC content of DNA substrates used in TPM experiments. Values were obtained using the bend.it server (263) with a window size of 31 and smoothed by adjacent averaging over 10 datapoints.

